Global Thermohaline Circulation. Part II: Sensitivity with Interactive Atmospheric Transports

XIAOLI WANG, PETER H. STONE, AND JOCHEM MAROTZKE

Center for Global Change Science, Massachusetts Institute of Technology, Cambridge, Massachusetts

(Manuscript received 15 July 1997, in final form 22 January 1998)

ABSTRACT

A hybrid coupled ocean–atmosphere model is used to investigate the stability of the thermohaline circulation (THC) to an increase in the surface freshwater forcing in the presence of interactive meridional transports in the atmosphere. The ocean component is the idealized global general circulation model used in Part I. The atmospheric model assumes fixed latitudinal structure of the heat and moisture transports, and the amplitudes are calculated separately for each hemisphere from the large-scale sea surface temperature (SST) and SST gradient, using parameterizations based on baroclinic stability theory. The ocean–atmosphere heat and freshwater exchanges are calculated as residuals of the steady-state atmospheric budgets.

Owing to the ocean component's weak heat transport, the model has too strong a meridional SST gradient when driven with observed atmospheric meridional transports. When the latter are made interactive, the conveyor belt circulation collapses. A flux adjustment is introduced in which the efficiency of the atmospheric transports is lowered to match the too low efficiency of the ocean component.

The feedbacks between the THC and both the atmospheric heat and moisture transports are positive, whether atmospheric transports are interactive in the Northern Hemisphere, the Southern Hemisphere, or both. However, the feedbacks operate differently in the Northern and Southern Hemispheres, because the Pacific THC dominates in the Southern Hemisphere, and deep water formation in the two hemispheres is negatively correlated. The feedbacks in the two hemispheres do not necessarily reinforce each other because they have opposite effects on low-latitude temperatures. The model is qualitatively similar in stability to one with conventional ''additive'' flux adjustment, but quantitatively more stable.

1. Introduction

The ocean's thermohaline circulation is driven by fluxes of heat and freshwater through the sea surface. Since the surface fluxes depend on the state of the atmosphere, the thermohaline circulation (THC) simulated by atmosphere–ocean coupled models has been the subject of extensive studies in recent years. The coupled models can be categorized into three classes, highly parameterized coupled box models (e.g., Nakamura et al. 1994; Marotzke and Stone 1995; Scott et al. 1999), fully coupled GCMs (e.g., Manabe and Stouffer 1988), and hybrid coupled models (e.g., Saravanan and McWilliams 1995; Rahmstorf and Willebrand 1995; Pierce et al. 1996; Lohmann et al. 1996). Among the three classes of coupled models, a prime limitation of the coupled box models is their crude representation of three-dimensional thermohaline circulation dynamics, whereas an important difficulty with the coupled GCMs is that it is hard to separate the individual contributions of different processes, and thus it is difficult to identify what is essential and what is of secondary importance. From this point of view, the hybrid coupled models are of great advantage for elucidating coupling processes between the thermohaline circulation and the atmosphere. Because they are usually of an intermediate level of complexity, the hybrid coupled models can provide guidelines for analyzing the behavior of more complex coupled GCMs.

Here, we develop such a hybrid coupled model, with a focus on the large-scale coupling processes between the thermohaline circulation and the extratropical atmospheric dynamics. The purpose is to identify feedbacks associated with the extratropical meridional transports in the atmosphere and the thermohaline circulation. These feedbacks have been examined in several previous hybrid coupled model studies. Rahmstorf and Willebrand (1995) used an ocean GCM coupled to an energy balance atmospheric model, and found that the thermohaline circulation sensitivity was significantly reduced in their hybrid coupled model, because the negative feedback between ocean temperature advection and THC was strengthened compared with a model with the traditional mixed boundary conditions. However, the hydrological cycle in their model was fixed to the di-

Corresponding author address: Jochem Marotzke, Room 54-1514, MIT, 77 Massachusetts Ave., Cambridge, MA 02139.
E-mail: jochem@sound.mit.edu

agnosed freshwater flux, and did not interact with equilibrium state changes. An interactive hydrological cycle is included in our model, and was also included in the hybrid coupled models of Saravanan and McWilliams (1995) and Lohmann et al. (1996). Our model is distinguished from the former in that we use a three-dimensional (3D) ocean GCM rather than a two-dimensional (2D) ocean model; in contrast, we employ a relatively simple atmospheric transport model whereas Saravanan and McWilliams (1995) used a two-layer 3D atmospheric model that included albedo changes. Our model differs from that of Lohmann et al. (1996) by the handling of the atmospheric hydrological cycle and the perturbation method. Our formulation of the atmospheric hydrological cycle was inspired by the work of Nakamura et al. (1994, hereafter NSM). We incorporate a coupling strategy similar to NSM's, but within the framework of a 3D global ocean GCM. Our perturbations are of global scale as well as long timescale, whereas the previous studies used only local perturbations with a short time duration (e.g., Saravanan and McWilliams 1995; Lohmann et al. 1996). We believe that the coupled feedbacks associated with the large-scale processes can best be elucidated by using the former kind of perturbation, since they are insensitive to localized perturbations.

Our coupled model is composed of an idealized global ocean GCM (OGCM) and an atmospheric energy and moisture balance model with nonlinear parameterizations of atmospheric transports of heat and moisture. In Part I (Wang et al. 1999), we have tested the global OGCM with fixed observed atmospheric meridional transports of heat and moisture. The integrations with these transports fixed serve as control runs for the experiments reported here. Here, we construct a series of coupled models with the highest stage being the coupled model with fully interactive atmospheric transports of heat and moisture.

Our intention is to identify large-scale interactions between the atmospheric transport processes and the thermohaline circulation. NSM described a destablizing feedback mechanism between the atmospheric moisture transport and the thermohaline circulation, named EMT feedback, which works as follows. A reduction in the thermohaline circulation leads to an increase in pole-to-equator temperature difference, which causes an increase in atmospheric moisture transport, which in turn leads to lower salinity at high latitudes and higher salinity at low latitudes. This increase in meridional salinity gradient brakes the thermohaline circulation even further, and a positive feedback loop is established. Since the thermohaline circulation is represented very crudely by three boxes in NSM, an important question is whether the same feedback acts in our intermediate model, as well as whether there are any new feedbacks emerging from the more complex model. Since flux adjustments are applied in our fully interactive model, another goal in this work is to investigate how different flux adjustment methods affect the strengths of the feedbacks, and therefore the climate sensitivity and stability of the thermohaline circulation. The hybrid model is decribed in section 2. The flux adjustment scheme and the experimental strategy are discussed in sections 3 and 4, respectively. A series of differently coupled models are perturbed, and the associated feedbacks are examined in section 5. Also two different flux adjustment methods are compared and assessed in section 5. The summary and conclusions follow in section 6.

2. Model description

The ocean model is essentially the same as that of Marotzke and Willebrand (1991). It is a coarse-resolution GCM, with simplified global geometry, consisting of two identical basins 60° of longitude wide (analogous to the Atlantic and Pacific Oceans) extending from 64°N to 64°S, and connected by an Antarctic Circumpolar Current (ACC) between 48°S and 64°S. There are 15 levels in the vertical; the bottom, at 4500-m depth, is flat; the latitudinal resolution is 4°; and the longitudinal resolution is 3.75°. Small-scale convection is parameterized using the scheme of Yin and Sarachik (1994). More details are given in Part I.

The atmospheric model is a zonally uniform, annual-mean model, with a simplified representation of the latitudinal variations of the fluxes of heat, moisture, and momentum. The surface wind stress is not interactive, but is specified based on observations, and includes a randomly varying component, also based on observations. We assume that the atmospheric heat and moisture capacities are negligible. Thus the surface heat flux is given by the divergence of the atmosphere's meridional heat transport, plus the net radiation at the top of the atmosphere. Similarly the surface freshwater flux equals the divergence of the atmosphere's meridional moisture transport. The net radiation at the top of the atmosphere is parameterized as a linear function of ocean surface temperature. (No albedo–temperature feedback is included.) More details of all these aspects of the atmospheric model can be found in Part I.

Previous studies have shown that the freshwater transport in high latitudes affects the thermohaline circulation stability and variability (e.g., Manabe and Stouffer 1994), whereas the freshwater transport in low latitudes has been shown to be of little importance to both the existence and the strength of the thermohaline circulation (e.g., Zaucker et al. 1994). As a result, the atmospheric transport mechanisms in low latitudes are not explicitly represented in this study. Rather, our focus is on the parameterization of eddy transports in high latitudes. In our parameterization of eddy transports, the latitudinal profiles of the atmospheric transports remain fixed, as in Part I. (See Part I for the profiles.) Only the amplitudes of the transport profiles are calculated by parameterizations of eddy transports at 35°N/S, respectively.

We assume that the transports by the mean circulation at 35°N/S are negligible, compared to transports by eddy activity, consistent with observations (Oort and Peixoto 1983). The eddy transports of heat and moisture are given by

$$H_d(35°) = 2\pi a \cos\phi \int_0^\infty [\rho_a(L_v\overline{v'q'} + C_p\overline{v'T'})]\, dz \tag{1}$$

$$F_w(35°) = 2\pi a \cos\phi \int_0^\infty [\rho_a\overline{v'q'}]\, dz, \tag{2}$$

where ρ_a is the atmospheric density; L_v is the latent heat of condensation; C_p is the specific heat of dry air at constant pressure; a is the radius of the earth; q is the specific humidity or mixing ratio; v and T represent the meridional velocity and the potential temperature, respectively; primes denote deviations from the time mean; and the overbar denotes a zonal and time mean.

The eddy sensible heat transport is parameterized based on baroclinic stability theory (Held 1978; Stone and Miller 1980),

$$\overline{v'T'} = A\left(\frac{\partial T}{\partial y}\right)^n, \tag{3}$$

whereas the eddy moisture transport is parameterized (Leovy 1973; Stone and Yao 1990) as

$$\overline{v'q'} = r_h\left(\frac{\partial q_s}{\partial T}\right)\overline{v'T'}, \tag{4}$$

$$q_s \approx 0.622\frac{2.53 \times 10^{11}}{P}e^{-(5420/T)}, \tag{5}$$

where q_s is the saturation mixing ratio and r_h is the relative humidity. The power law of the meridional transports depends on both latitude and static stability (Held 1978; Branscome 1983; Stone and Yao 1990). Empirically, n is found to vary with latitude in the range from 1.6 to 4 (Stone and Miller 1980). Here, we choose a value appropriate for 35°N, where the poleward heat transport is a maximum, that is, $n = 2.5$. Changing n would not affect our results qualitatively.

Combining the constants together and assuming that the vertical temperature dependence is fixed, we can rearrange the parameterizations and approximate them by

$$H_d(35°) = (C_S + C_L e^{(-5420/T)})\left(\frac{\partial T}{\partial y}\right)^n, \tag{6}$$

$$F_w(35°) = C_F e^{(-5420/T)}\left(\frac{\partial T}{\partial y}\right)^n, \tag{7}$$

where T now represents the surface temperature. The coefficient C_S represents the eddy sensible heat transport. The eddy moisture transport, and thus the eddy latent heat transport, are given by the coefficient C_F. (Note that $C_L = L_v C_F$.) In calculating the surface fluxes per unit area into the ocean we need to take into account that the area of the oceans in our model is only one-third the area of the globe (except in the ACC). Thus the surface heat flux calculated as the residual of the atmosphere's heat budget per unit area of the globe must be multiplied by 3 (except in the ACC), because the net surface heat flux over land must be zero, and all the residual must be taken up by the ocean. Similarly the surface moisture flux per unit area into the ocean is multiplied by 1.5 (except in the ACC) as in the control run in Part I. This enhancement of the net precipitation minus evaporation over the ocean can be thought of as being due to a modest amount of river runoff from land areas (see Part I).

Both the transports of sensible and latent heat depend on a power of the meridional temperature gradient at 35°N/S, whereas the latent heat and moisture transports are affected by the temperature itself at 35°N/S, through the Clausius–Clapeyron equation [Eq. (5)]. Thus the ocean influences the atmosphere by affecting both the temperature and its gradient, and therefore the transports at 35°N/S. In the eddy transport formulas [Eq. (6) and (7)], we use an atmospheric latitudinal temperature profile determined by the sea surface temperature (SST) field in the oceanic model:

$$T = T_0 + \frac{1}{2}T_2(3\sin^2\phi - 1), \tag{8}$$

where ϕ is latitude. The polynomial coefficients (T_0 and T_2) are determined separately in the Northern Hemisphere (NH) and Southern Hemisphere (SH) by assuming that the area-weighted SST over two latitude ranges (0°–35°, 35°–64°) are equal to the same averaged atmospheric temperature. The reason for such an area-weighted average approach is that the typical meridional scales of eddies that transport heat are 20°–30° (Stone 1984), and the transport should not respond to smaller-scale structure in SST.

The coupling procedure can be summarized as follows:

> Changing the thermohaline circulation → changes in the SST field → changes in the atmospheric temperature and its meridional gradient at 35°N/S → changes in the atmospheric heat/moisture transports → changes in the surface heat–freshwater fluxes → further changes in the thermohaline circulation.

3. Flux adjustment

In the fully interactive model, the meridional transports of heat and freshwater in the atmosphere are no longer held fixed, as in Part I, but are determined interactively by the parameterizations. The initial state of the interactive model is taken from the conveyor belt

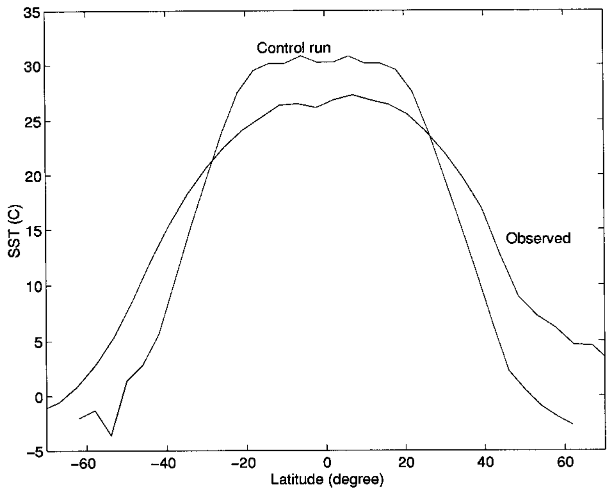

FIG. 1. The zonal-mean SST in the control run and the observed SST (in °C), as a function of latitude.

equilibrium state of the control run (with $\mu = 1.5$) from Part I. Upon coupling, the interactive model immediately drifts away, and settles down to a new state without deep water formation in either basin.

The drift of the fully interactive model is not surprising. The surface forcings from the two models are apparently incompatible, and the discrepancy results from the difference between the modeled SST and the observed SST (Levitus 1982). As Fig. 1 shows, the meridional gradient of the zonal-mean SST in the control run is stronger than that of the observed SST. Therefore, the modeled atmospheric eddy transports, which are proportional to the 2.5th power of the modeled temperature gradient [Eq. (3)], are too strong, compared to the observed values. As a result, the interactive model drifts away under the excessive atmospheric heat–freshwater fluxes.

The strong meridional gradient of the modeled SST arises because of the model's weak oceanic heat transport, which in the control run is only about half of the observed values, for example, a peak value of 0.7 PW in the NH versus the observed value of 1.5 ± 0.3 PW (Macdonald and Wunsch 1996). In the control run, the ocean GCM is forced with the observed atmospheric heat transport, and, if the net radiation were also fixed from observations, the GCM would have transported (approximately) the observed amount of heat transport in the ocean. However, in the control run the longwave radiation is not fixed, but parameterized as a linear function of the modeled SST, so the model can compensate its low oceanic heat transport by obtaining a much stronger meridional gradient of SST, and hence a stronger differential radiative forcing.

Fundamentally, the drift of the fully interactive model results from the weakness of the ocean model's poleward heat transport. This can be attributed to several defects of the GCM; among them are the coarse horizontal resolution, the low North Atlantic Deep Water formation rate, and the diffusive mixing scheme in the western boundary. Without improving the oceanic heat transport, we have to use flux adjustments to prevent the drift of the interactive model.

The flux adjustment developed here is based on the observation that the atmosphere and the ocean actually are comparable in their meridional heat transports (Trenberth and Solomon 1994). To preserve this character, we adjust the atmospheric heat transport *efficiency* to better match the oceanic one, so that the two models can have more comparable heat transport efficiencies. This approach is different from the conventional flux adjustment (e.g., Sausen et al. 1988; Manabe and Stouffer 1988; Murphy 1995), in which the surface fluxes are adjusted by additive constants. We believe that the efficiency adjustment serves better for the purpose of this work, because preserving the relative transport efficiency of the two models should help recover a realistic balance between the contributions of the atmosphere and the thermohaline circulation to their mutual interaction (see Marotzke and Stone 1995). Indeed, Krasovskiy and Stone (1998) have shown that this is the case in a coupled atmosphere–ocean box model of the THC. They found, when their model's ocean heat transport efficiency was underestimated, that the model's stability characteristics could nevertheless be preserved by a reduction in the atmospheric transport efficiencies. A further assessment of the two flux adjustment schemes will be deferred to section 5d.

To adjust the heat transport efficiency of the atmospheric model, we tune the coefficients in the parameterizations, to give the observed atmospheric heat and freshwater transports, when the SST of the control run, $T_{\rm model}$, is used rather than the observed SST, $T_{\rm obs}$:

$$\begin{aligned} H_d(35°)_{\rm obs} &\equiv \left[C_S + C_L\left(\frac{\partial q_s}{\partial T}\right)\right]\left(\frac{dT_{\rm obs}}{dy}\right)^n \\ &= \left[C'_S + C'_L\left(\frac{\partial q_s}{\partial T}\right)\right]\left(\frac{dT_{\rm model}}{dy}\right)^n \end{aligned} \tag{9}$$

and

$$\begin{aligned} F_w(35°)_{\rm obs} &\equiv C_F\left(\frac{\partial q_s}{\partial T}\right)\left(\frac{dT_{\rm obs}}{dy}\right)^n \\ &= C'_F\left(\frac{\partial q_s}{\partial T}\right)\left(\frac{dT_{\rm model}}{dy}\right)^n \end{aligned} \tag{10}$$

(note that $C'_L = L_v C'_F$). The adjusted coefficients (C'_F and C'_S) are about 30% of the original ones. After the adjustments, the surface forcings from the fully interactive model are the same as those from the (noninteractive) control run, and therefore, the equilibrium state of the model remains the same upon coupling. The same flux adjustment is applied in all the following feedback experiments.

TABLE 1. Designations of the different coupled models. Here H_d and F_w indicate the atmospheric heat and freshwater transports, respectively.

	H_d interactive	F_w interactive	H_d and F_w interactive
Only NH interactive	H1	F1	HF1
Only SH interactive	H2	F2	HF2
NH and SH interactive	H3	F3	HF3

4. Experimental strategy

We will investigate a total of nine different coupled models, listed in Table 1. Models H1–3 have only the atmospheric heat transport interactive, in the NH, SH, and both hemispheres, respectively. Models F1–3 are similar to the models H1–3, except that now the atmospheric freshwater transport is interactive, instead of the heat transport. Both transports become interactive in the models HF1–3. Generally, a negative (positive) feedback is present when a perturbation weakens (enhances) itself through the changes it causes. To elucidate feedbacks in the coupled models, all the nine coupled models are subjected to an external perturbation of a linear increase in the global hydrological cycle by an amount equal to 0.1% of its initial value per year. That is, the moisture transport coefficient increases linearly in time, but the latent heat transport as well as the total heat transport remains unchanged.

Under such an external perturbation, with the noninteractive model, the conveyor belt overturning circulation collapses to the ‘‘southern Sinking’’ state after several hundred years (see Part I). To objectively compare the collapse times of the North Atlantic overturning, we apply a 10-yr running mean filter to the time series of the North Atlantic overturning strength. The choice of a 10-yr window is governed by the desire to eliminate the high-frequency variability induced by the random wind-forcing component, while maintaining the full resolution for the timescales of interest. The criterion for the collapse time is defined, somewhat arbitrarily, as the time when the North Atlantic overturning strength falls below 6 Sv (Sv $\equiv 10^6$ m^3 s^{-1}). (The equilibrium value with no perturbation is 18 Sv.) Here, the strategy is to examine how feedbacks modify the collapse time of each model. The shorter the collapse time, the less stable is the model. Furthermore, an identical initial random wind stress is used in all the experiments to exclude the possible effects of different initial conditions (see Part I).

5. Feedbacks in the coupled models

The feedbacks associated with interactive atmospheric transports of heat and moisture have been studied using the box models (NSM, Marotzke and Stone 1995; Marotzke 1996). Note that all these models were *hemispheric* models. Here we want to assess how robust the feedbacks in the simple box model are in the framework of a complex global ocean GCM. Notice that the box model results are applicable to the NH feedbacks in the GCM; SH feedbacks are discussed below.

a. Feedback associated with atmospheric heat transport

As discussed in Marotzke (1996), in the hemispheric box models (which represent the Northern Hemisphere), there is a positive feedback between the atmospheric heat transport and the THC. It involves the fundamental negative feedback in the *atmosphere* between the meridional temperature gradient and eddy heat transport. The positive feedback works as follows:

> Decreased overturning $\rightarrow$ increased SST gradient $\rightarrow$ increased atmospheric heat transport $\rightarrow$ warming of high-latitude waters $\rightarrow$ further decreased overturning.

The anomalous atmospheric heat transport tends to damp out the change of SST meridional gradient, which limits the power of the negative feedback between oceanic temperature advection and temperature gradient; therefore, it acts as a positive feedback for the thermohaline circulation.

To examine this feedback in the GCM, the perturbations are applied to the coupled models with the feedback (models H1–3) and the control run without it (the noninteractive model). The filtered time series of North Atlantic overturning in these models are plotted in Fig. 2, which shows that the collapse times of the models with the feedback are, on the average, about 200 yr shorter than that of the model without the feedback. The precise collapse times, as defined above, are given in Table 2. This demonstrates that the atmospheric heat transport feedback identified in the box models acts in a similar fashion in the GCM.

However, we note that the feedback loop described above is correct only in the NH. In the SH, a new feedback loop can be identified, which differs from the feedback loop above in two places, and works as follows:

> Decreased North Atlantic overturning $\rightarrow$ increased SH overturning $\rightarrow$ increased SH oceanic heat transport $\rightarrow$ reduced SH meridional SST gradient $\rightarrow$ reduced SH atmospheric heat transport $\rightarrow$ cooling of high-latitude waters $\rightarrow$ increase of surface density in high SH latitudes $\rightarrow$ reduction of *upwelling*

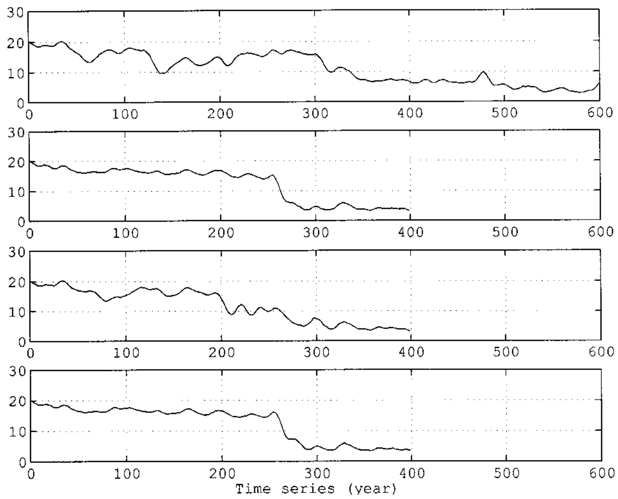

FIG. 2. Filtered time series of the North Atlantic overturning strength (vertical axis in Sv). (top) Noninteractive model. (upper-middle) H_d interactive in the NH only. (lower-middle) H_d interactive in the SH only. (bottom) H_d interactive in both hemispheres.

in high SH latitudes → further decreased North Atlantic overturning.

The first difference between the two feedback loops is that the North Atlantic overturning upwells in the SH, and hence is reduced as SH surface density increases. The second difference arises from the way the SH meridional SST gradient is influenced. As North Atlantic overturning decreases, the shallow overturning cells in the SH, both in the Atlantic and the Pacific (which dominates SH ocean heat transport, Part I), increase in strength. This statement is based on the recent result that North Atlantic overturning strength is sensitive to, for example, freshwater flux forcing, but the global integral in deep and bottom water formation rate is not (Tziperman 1997; Klinger and Marotzke 1999; Part I). If we postulate that this compensation generally holds, reduced North Atlantic overturning leads to increased SH (poleward) heat transport and smaller SST gradient. Due to these changes, the atmospheric heat transport feedback still counteracts the negative oceanic temperature advection feedback in the SH: therefore, it is positive. From the criteria of the collapse time, the feedback strength in each hemisphere is quantitatively similar (see Table 2). However, the temporal variations of the overturning are not the same in each model. For example, the model with the feedback in the SH hovers near 10 Sv (an intermediate equilibrium) for about 80 years before collapsing, whereas the other models (H1 and H3) maintain the original state, then collapse within 20 yr (Fig. 2).

We note that the model with both hemisphere's positive feedbacks combined does not become less stable than the model with only one hemisphere's positive feedback. This can be explained by the interaction between the two hemispheres. Suppose we consider the SH interaction to be added to the NH interaction. As the overturning decreases, the SST meridional gradient in the SH decreases, the atmosphere's meridional heat transport in the SH decreases, and low latitudes warm up. This counteracts the low-latitude cooling due to the increased atmospheric heat transport in the NH. Thus adding the positive feedback in the SH weakens that in the NH, and thus the collapse time, as defined, hardly changes.

TABLE 2. Collapse times in the coupled models when the freshwater flux increases in both hemispheres. Here H_d and F_w indicate the atmospheric heat and freshwater transports, respectively.

	H_d interactive	F_w interactive	H_d and F_w interactive
Noninteractive	490	490	490
Only NH interactive	270	240	170
Only SH interactive	280	240	310
NH and SH interactive	280	240	280

In sum, the feedback associated with the atmospheric heat transport found in the box models is also identifiable in the GCM, but it works differently in the NH and SH. The feedbacks in the two hemispheres interact, and weaken each other, but still act jointly as a positive feedback.

b. *Feedback associated with atmospheric moisture transport*

The positive feedback between atmospheric meridional moisture transport and the THC, named EMT feedback by NSM, operates in the hemispheric box models as follows:

Decreased overturning → reduced northward oceanic heat transport → increased meridional SST gradient → increased atmospheric moisture transport → reduced surface salinity in high latitudes → reduced surface density in high latitudes → further decreased overturning.

In effect, this feedback destabilizes the thermohaline circulation by enhancing the positive oceanic salinity advection feedback. Once again, one would expect a similar feedback in the NH of our model. Figure 3 displays the temporal variations of the North Atlantic overturning in the models with the atmospheric moisture transport feedback, and in the control run without. The collapse time in all those with the feedback is about 250 yr shorter than in that without the feedback (see Table 2). Thus the feedback associated with the atmospheric moisture transport is also positive in our model, whichever hemisphere is involved.

However, the feedback in the SH can again be seen to differ from that in the NH, although it is still positive. It operates as follows:

Decreased North Atlantic overturning → increased SH overturning → increased SH oceanic heat trans-

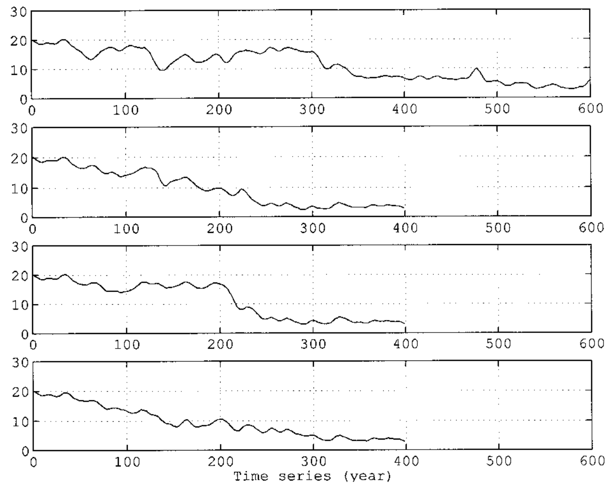

FIG. 3. Filtered time series of the North Atlantic overturning strength (vertical axes in Sv). (top) Noninteractive model. (upper-middle) F_w interactive in the NH. (lower-middle) F_w interactive in the SH. (bottom) F_w interactive in both hemispheres.

port → reduced SH meridional SST gradient → reduced SH atmospheric moisture transport → increased surface salinity in high latitudes → reduced upwelling in high SH latitudes → further decreased overturning in the Atlantic.

Once again, when the feedbacks in both hemispheres are combined, there is no additional destabilization, because of the interaction between the two hemispheres (see Table 2 and Fig. 3).

Since the latitudinal profile of the moisture transport is prescribed in this study, small-scale changes in the moisture transport in high latitudes are not captured in our model. Lohmann et al. (1996) found that, when local temperature effects are included, the moisture transport feedback is weaker than that in NSM. However, studies with coupled atmospheric GCMs (e.g., Schiller et al. 1997) have indeed observed moisture transport changes due to large-scale changes in the temperature gradient that confirm the existence of this feedback in the coupled system.

c. *Feedbacks associated with both atmospheric transports*

Table 2 also shows the collapse times when both the atmospheric meridional transports of heat and moisture are made interactive (models HF1 to HF3). In the box models, adding the feedback between atmospheric heat transport and the THC to the feedback between atmospheric moisture transport and the THC can be either stabilizing or destabilizing, because of two competing effects (Marotzke and Stone 1995; Marotzke 1996). Adding a new positive feedback is per se destabilizing, but the feedback between atmospheric heat transport and meridional temperature gradient, which is negative when viewed in isolation, also constrains changes in temperature gradient. This latter effect weakens the positive feedback between the atmospheric moisture transport and the THC and is therefore stabilizing. The results in Table 2 show that the destabilizing effect dominates in the NH, but the stabilizing effect dominates in the SH.

When both hemispheres are interactive, there is also some stabilization, both through the interaction of the atmospheric heat and moisture transports (row 4 in Table 2) and through the interaction between the hemispheres (column 3 in Table 2). The latter is analogous to the case discussed for atmospheric heat fluxes alone, at the end of subsection 5a. Notice that despite the two types of stabilizing interaction between positive feedbacks, the fully coupled model (HF3) remains considerably less stable than the model with fixed atmospheric transports of heat and moisture.

d. *Effects of different flux adjustment schemes*

To evaluate the effects of our flux adjustment scheme, we construct a different flux adjustment scheme, similar to that used in coupled GCMs, in which the surface fluxes are adjusted by constants. We call it an *additive* flux adjustment. The additive flux adjustment does not change the atmospheric transport efficiencies, but subtracts constant surface fluxes to match the observed surface fluxes. The same result is achieved by subtracting a constant from our parameterizations for the magnitude of the atmospheric transports. For example, Eq. (8) is replaced by

$$H_d(35°)_{\text{obs}} = \left[C_S + C_L\left(\frac{\partial q_s}{\partial T}\right)\right]\left(\frac{dT_{\text{model}}}{dy}\right)^n - \text{const.} \qquad (11)$$

In our scheme, the atmospheric transport efficiencies are multiplied by constants; therefore, we call it an *efficiency adjustment.*

Our primary concern is whether the conclusions of this section will be altered if the additive scheme is used. Thus we repeated several of our experiments, but now using the additive scheme. We found that, qualitatively, our results were not affected. However, the feedback strengths are sensitive to the adjustment schemes. For example, Fig. 4 shows the evolution of the North Atlantic overturning when the global freshwater fluxes increase linearly in time, using the two different flux adjustment schemes. The model with the additive flux adjustment is less stable than that with the efficiency adjustment, for the latter reduces the atmospheric transport efficiencies, and therefore reduces the positive atmospheric transport feedbacks. This result is consistent with Marotzke and Stone's (1995) and Krasovskiy and Stone's (1998) analysis of the coupled box model, which showed that using an additive flux adjustment to correct an underestimate of their model ocean's heat transport led to a model that was too unstable. Krasovskiy and Stone (1998) showed that using an appropriate effi-

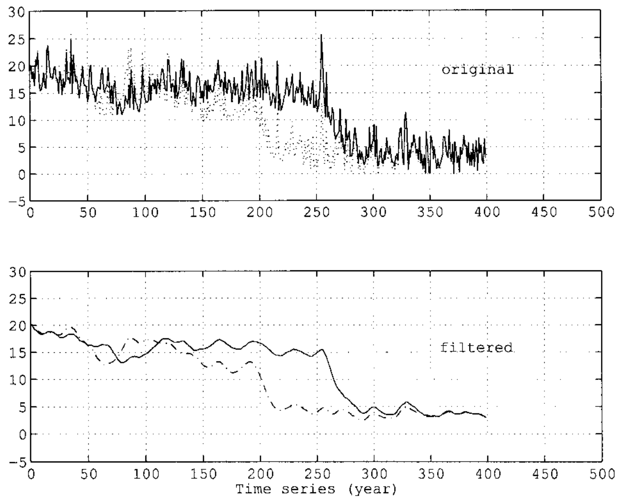

FIG. 4. Time series of the North Atlantic overturning strength (vertical axes in Sv) in the fully interactive model, with the additive flux adjustment (dashed), and the efficiency adjustment (solid), when the global freshwater fluxes increase linearly. (top) Unfiltered time series. (bottom) Filtered time series.

ciency adjustment, similar to ours, would preserve the correct stability properties of their model. However, although the efficiency adjustment we have used does indeed produce a more stable model than the additive adjustment scheme, there is no guarantee that it has yet achieved the correct degree of stability.

6. Summary and conclusions

A series of coupled models has been developed, corresponding to different stages of ocean–atmosphere coupling. When the atmospheric transports are made interactive, the coupled model drifts away from the conveyor belt circulation of the control run, which is forced by the observed atmospheric transports of heat and moisture. The basic cause of the collapse is the ocean model's underestimate of the poleward heat transport. Because of it, the meridional temperature gradients are too strong. Thus when the atmospheric transports are made interactive, the too-strong gradients produce atmospheric transports that are also too strong, so strong that surface waters in the high latitudes of the North Atlantic are sufficiently freshened and made warmer by the atmospheric fluxes that the deep water formation there is completely turned off. This is in fact a possible explanation of why the overturning collapses in some coupled GCMs if no flux adjustments are used (e.g., Manabe and Stouffer 1988).

To prevent the drift of the coupled model, the atmospheric transport parameterizations are tuned, so that the parameterizations produce the observed atmospheric transports when the temperature structure of the noninteractive coupled model is used to calculate the transports, rather than when the observed temperature structure is used. In effect, this introduces errors in the efficiencies of the atmospheric transports, which are matched to the errors in the efficiencies of the oceanic transports, and thereby preserves a realistic balance between the atmospheric and oceanic processes. This efficiency adjustment is quite different from the conventional additive adjustment used in coupled GCMs, where specified latitudinally dependent constants are added to the surface fluxes and held fixed. However, our results indicate that the coupled feedbacks are qualitatively similar with either of the adjustment schemes. Nevertheless, the stability of the THC is affected by the flux adjustment scheme that is used, and, based on Krasovskiy and Stone's (1998) analysis, we consider our scheme to be superior.

The coupled feedbacks associated with the meridional transports in the atmosphere that were identified in the box models (NSM; Marotzke and Stone 1995; Marotzke 1996) are found to operate in a similar fashion in our ocean GCM. However, the feedback loops operate differently in the SH from those in the NH although they have the same signs. The differences arise from the dominance of the Pacific THC in the SH, as well as the negative correlation between deep water formation in the two hemispheres. The feedback loop in the SH acts as follows:

> Decreased North Atlantic overturning → increased SH overturning → increased SH oceanic heat transport → reduced SH meridional SST gradient → reduced SH atmospheric heat and moisture transports → reduced buoyancy in SH high latitudes → reduced *upwelling* in high SH latitudes → further decreased overturning in the Atlantic.

Thus the feedbacks between both the atmospheric heat and moisture fluxes and the conveyor belt state of the THC are positive in both hemispheres. However, although any combination of these four feedbacks makes the model less stable than the model with fixed atmospheric transport, a superposition of two feedbacks may well be less destabilizing than either feedback acting in isolation. This is because the feedbacks in the NH interact with those in the SH, since both involve the low-latitude SST; this interaction weakens the feedbacks. Moreover, within each hemisphere, the feedback between the THC and the atmospheric heat transport weakens the feedback between the THC and the atmospheric moisture transport. One cannot generally predict whether a certain superposition of positive feedbacks stabilizes or further destabilizes. In our model, the most unstable combination of feedbacks is the one with the Northern Hemisphere atmospheric transports interactive and the Southern Hemisphere transports fixed. Thus, the single-hemisphere box model of NSM indeed analyzed the strongest coupled feedbacks in our idealized global hybrid GCM.

Acknowledgments. We are indebted to Jeffery Scott for many useful discussions and comments, especially for pointing out the importance of the interaction between NH and SH feedbacks. Sixty percent ($46,000) of this research was funded jointly by the U.S. Department of Energy's (DoE) National Institute for Global Environmental Change (NIGEC) through the NIGEC Northeast Regional Center at Harvard University (DoE Cooperative Agreement DE-FC03-90ER61010) and by the DoE's Program for Computer Hardware, Applied Mathematics, and Model Physics. Financial support was also contributed by the Tokyo Electric Power Company (TEPCO) through the TEPCO–MIT Environmental Research Program and by the MIT Joint Program (JP) on the Science and Policy of Global Change. Financial support does not constitute an endorsement by DoE, TEPCO, or the JP of the views expressed in this article.

REFERENCES

Branscome, L. E., 1983: A parameterization of transient eddy heat flux on a beta-plane. *J. Atmos. Sci.,* **40,** 2508–2521.

Held, I. M., 1978: The vertical scale of an unstable baroclinic wave and its importance for eddy heat flux parameterizations. *J. Atmos. Sci.,* **35,** 572–576.

Klinger, B. A., and J. Marotzke, 1999: Behavior of double hemisphere thermohaline flows in a single basin. *J. Phys. Oceanogr.,* in press.

Krasovskiy, Y., and P. H. Stone, 1998: Destabilization of the thermohaline circulation by atmospheric transports: An analytic solution. *J. Climate,* **11,** 1803–1811.

Leovy, C. B., 1973: Exchange of water vapor between the atmosphere and surface of Mars. *Icarus,* **18,** 120–125.

Levitus, S., 1982: *Climatological Atlas of the World Ocean.* NOAA Professional Paper 13, U.S., Dept. of Commerce, NOAA, Washington, DC, 173 pp.

Lohmann, G., R. Gerdes, and D. Chen, 1996: Sensitivity of the thermohaline circulation in coupled oceanic GCM-atmospheric EBM experiments. *Climate Dyn.,* **12,** 403–416.

Macdonald, A. M., and C. Wunsch, 1996: An estimate of global ocean circulation and heat fluxes. *Nature.,* **382,** 436–439.

Manabe, S., and R. Stouffer, 1988: Two stable equilibria of a coupled ocean–atmosphere model. *J. Climate,* **1,** 841–866.

——, and ——, 1994: Multiple-century response of a coupled ocean–atmosphere model to an increase of atmospheric carbon dioxide. *J. Climate,* **7,** 5–23.

Marotzke, J., 1996: Analysis of thermohaline feedbacks. *Decadal Climate Variability, Dynamics and Predictability,* D. L. T. Anderson and J. Willebrand, Eds., Vol. 144, NATO ASI Series, 333–378.

——, and J. Willebrand, 1991: Multiple equilibria of the global thermohaline circulation. *J. Phys. Oceanogr.,* **21,** 1372–1385.

——, and P. H. Stone, 1995: Atmospheric transports, the thermohaline circulation, and flux adjustments in a simple coupled model. *J. Phys. Oceanogr.,* **25,** 1350–1364.

Murphy, J. M., 1995: Transient response of the Hadley Center Coupled Ocean–Atmosphere Model to increasing carbon dioxide. Part I: Control climate and flux adjustment. *J. Climate,* **8,** 36–56.

Nakamura, M., P. H. Stone, and J. Marotzke, 1994: Destabilization of the thermohaline circulation by atmospheric eddy transports. *J. Climate,* **7,** 1870–1882.

Oort, A. H., and J.P. Peixoto, 1983: Global angular momentum and energy balance requirements from observations. *Advances in Geophysics,* Vol. 25, Academic Press, 355–490.

Pierce, D. W., K. Y. Kim, and T. P. Barnett, 1996: Variability of the thermohaline circulation in an ocean general circulation model coupled to an atmospheric energy balance model. *J. Phys. Oceanogr.,* **26,** 725–738.

Rahmstorf, S., and J. Willebrand, 1995: The role of temperature feedback in stabilizing the thermohaline circulation. *J. Phys. Oceanogr.,* **25,** 787–805.

Saravanan, R., and J. C. McWilliams, 1995: Multiple equilibria, natural variability, and climate transitions in an idealized ocean–atmosphere model. *J. Climate,* **8,** 2296–2323.

Sausen, R., R. K. Barthels, and K. Hasselmann, 1988: Coupled ocean–atmosphere models with flux correction. *Climate Dyn.,* **2,** 154–163.

Schiller, A., U. Mikolajewicz, and R. Voss, 1997: The stability of the thermohaline circulation in a coupled ocean–atmosphere general circulation model. *Climate Dyn.,* **13,** 325–347.

Scott, J., P. H. Stone, and J. Marotzke, 1999: Interhemispheric thermohaline circulation in a coupled box model. *J. Phys. Oceanogr.,* in press.

Stone, P. H., 1984: Feedbacks between dynamical heat fluxes and temperature structure in the atmosphere. *Climate Processes and Climate Sensitivity, Geophys. Monogr.,* No. 29, American Geophysical Union, 6–17.

——, and D. A. Miller, 1980: Empirical relations between seasonal changes in meridional temperature gradients and meridional fluxes of heat. *J. Atmos. Sci.,* **37,** 1708–1721.

——, and M. S. Yao, 1990: Development of a two-dimensional zonally averaged statistical-dynamical model. Part III: The parameterization of the eddy fluxes of heat and moisture. *J. Climate,* **3,** 726–740.

Trenberth, K. E., and A. Solomon, 1994: The global heat balance: Heat transports in the atmosphere and ocean. *Climate Dyn.,* **10,** 107–134.

Tziperman, E., 1997: Inherently unstable climate behavior due to weak thermohaline ocean circulation. *Nature,* **386,** 592–595.

Wang, X., P. H. Stone, and J. Marotzke, 1999: Global thermohaline circulation. Part I: Sensitivity to atmospheric moisture transport. *J. Climate,* **12,** 71–82.

Yin, F. L., and E. S. Sarachik, 1994: An efficient convection adjustment scheme for ocean general circulation models. *J. Phys. Oceanogr.,* **24,** 1425–1430.

Zaucker, F., T. F. Stocker, and W. S. Broecker, 1994: Atmospheric freshwater fluxes and their effect on the global thermohaline circulation. *J. Geophys. Res.,* **99,** 12 443–12 457.